Electronic Supplementary Information for Dalton Transactions

Cobalt(II) complexes of terpyridine bases as photochemotherapeutic agents showing cellular uptake and photocytotoxicity in visible light

Sovan Roy,[a] Subhendu Roy,[a] Sounik Saha,[a] Ritankar Majumdar,[b] Rajan R. Dighe,[b] Eluvathingal D. Jemmis,*[a,c] and Akhil R. Chakravarty*[a]

[a] *Department of Inorganic and Physical Chemistry,*

[b] *Department of Molecular Reproduction, Development and Genetics, Indian Institute of Science, Bangalore 560012, India.*

[c] *Indian Institute of Science Education and Research Thiruvananthapuram, Thiruvananthapuram-695016, India.*

Supporting information

Experimental Section.

DNA binding experiments.

The interaction of the complexes with calf thymus (CT) DNA was studied in 5 mM Tris-HCl buffer (pH 7.2) at 25 °C. Thermal denaturation studies were done in melting-buffer consisting of 5 mM Na_2HPO_4, 5 mM NaH_2PO_4, 1 mM Na_2EDTA and 5 mM NaCl. A solution of CT DNA in the buffer gave a ratio of UV absorbance at 260 and 280 nm of about 1.9:1 indicating CT DNA sufficiently free from protein.[1] Using the ε value of 6600 $dm^3\ mol^{-1}\ cm^{-1}$ at 260 nm, the concentration of CT DNA was measured.[2] In absorption titration experiments, the concentration of CT DNA was varied keeping the complex concentration as constant (20 μM). Sample equilibration was done for 3 min before recording the spectra. The intrinsic equilibrium binding constant (K_b) values of the complexes to CT DNA were obtained from the electronic spectral data by McGhee-von Hippel (MvH) method using the expression of Bard and co-workers (eq. 1).[3,4] The change in the absorption intensity of the charge-transfer spectral band at 287 nm for **1**, 261 nm for **2** and 276 nm for **3** was monitored with increasing concentration of CT DNA. Due correction was made for the absorbance of CT DNA itself by adding CT DNA in the reference cuvette. The K_b value was obtained by regression analysis of the data using the equation:

$$(\varepsilon_a - \varepsilon_f)/(\varepsilon_b - \varepsilon_f) = (b - (b^2 - 2K_b{}^2C_t[\mathrm{DNA}]/s)^{1/2})/2K_bC_t \quad \ldots (1)$$

where $b = 1 + K_bC_t + K_b[\mathrm{DNA}]/2s$ and ε_a is the extinction coefficient observed for the spectral band at a given DNA concentration, ε_f is the extinction coefficient of the complex free in solution, ε_b is the extinction coefficient of the complex when fully bound to DNA, K_b is the equilibrium binding constant, C_t is the total complex concentration,

[DNA] is the DNA concentration in nucleotides and *s* is the fitting parameter giving an estimate of the binding site size in base pairs. The non-linear least-squares analysis was done using Origin Lab, version 7.5.

DNA melting experiments were carried out by monitoring the absorption intensity of CT DNA (174 μM) at 260 nm at various temperatures, both in the absence and presence of the metal complexes (20 μM), using a Perkin-Elmer Lambda 35 spectrophotometer equipped with a Peltier temperature-controlling programmer (PTP 6) (±0.1 °C) on increasing the temperature of the solution at 0.25 °C per min.[5] Viscometric titrations were performed using Schott AVS 370 Automated Viscometer at 37±0.1 ºC. The concentration of CT DNA was 165 μM in NP (nucleotide pairs) and the flow times were measured with an automated timer. Three measurements were taken for each sample to calculate the average flow time. Data were presented as $(\eta/\eta_0)^{1/3}$ vs. [complex]/[DNA], where η is the viscosity of DNA in the presence of the complex and η_0 that of DNA alone.[6] Viscosity values were calculated from the observed flowing time of DNA-containing solutions (t) corrected for that of buffer alone (t_0), $\eta = (t - t_0)/t_0$.

DNA cleavage experiments

The photo-induced cleavage of supercoiled (SC) pUC19 DNA by the cobalt(II) complexes **1-3** was investigated by agarose gel electrophoresis. The reactions were carried out using a UV-A lamp of 365 nm (6 W, sample area of illumination: 45 mm^2) and in visible light of 514, 569 and 647 nm using a continuous-wave (CW) Argon-Krypton laser. Agarose gel electrophoresis was done to determine the extent of cleavage of SC DNA by the metal complexes in 50 mM Tris-HCl buffer containing 10% DMF and 50 mM NaCl (pH 7.2). The photo-induced DNA cleavage studies were carried out under

illuminated conditions using UV-A light of 365 nm wavelength (6 W, Bangalore Genie make) and visible light laser of different wavelengths (Spectra Physics Water-Cooled Mixed-Gas Ion Laser Stabilite® 2018-RM with beam diameter at $1/e^2$ 1.8 mm ±10% and beam divergence with full angle 0.70 mrad ±10%). Each sample was incubated for 15 min at 37 °C prior to photo-exposure with a solution path-length of 5 mm placed at a distance of 10 cm from the light source. The power of the laser beam at the sample position was measured using Spectra Physics CW Laser Power Meter (Model 407A). The laser powers at 514, 569 and 647.1 nm are 100, 50, 100 mW, respectively. Following light exposure, each sample was incubated for 15 min at 37 °C and subjected to gel electrophoresis. Mechanistic studies were done using different reagents, *viz.* NaN_3, 200 μM; DABCO, 200 μM; DMSO, 4 μL and KI, 200 μM. For the D_2O experiment, this solvent was used for dilution of the sample to a volume of 20 μL. The samples were added to the loading buffer containing 0.25% bromophenol blue, 0.25% xylene cyanol and 30% glycerol (3 μL) after incubation in a dark chamber and the solution was finally loaded on 1.0% agarose gel containing 1.0 μg/mL ethidium bromide. Electrophoresis was carried out in a dark room for 2.0 h at 60 V in TAE (Tris-acetate EDTA) buffer. UV light was used for visualization of the bands. The extent of DNA cleavage was measured from the intensities of the bands using UVITEC Gel Documentation System. Due corrections were made for the low level of nicked circular (NC) form present in the original supercoiled (SC) DNA sample and for the low affinity of ethidium bromide binding to SC compared to NC and linear forms of DNA.[7] The concentrations of the complexes and reagents corresponded to the quantity of the sample after dilution to the 20 μL final

volume with Tris-HCl buffer. The observed error in measuring the band intensities ranged between 3-7%.

Protein interaction and cleavage experiments

Using bovine serum albumin (BSA, 2 μM) as substrate in phosphate buffer (pH 6.8), the interaction of the complexes with protein was studied from tryptophan fluorescence quenching experiments. Quenching of the emission intensity of tryptophan residues of BSA at 344 nm (excitation wavelength at 295 nm) was monitored using complexes **1 - 3** as quenchers with increasing complex concentration.[8] The quenching constant (K_{BSA}) values were obtained from Stern-Volmer plot where I_0/I was plotted against complex concentration: $(I_0/I) = 1 + K_{BSA}$ x [complex], where I_0 and I are the emission intensities of BSA in the absence and presence of the quencher.

The photoinduced BSA cleavage activity has been studied by following the literature procedure.[9] The photo-induced protein cleavage studies were done using freshly prepared solution of BSA in 50 mM Tris-HCl buffer (pH 7.2). The protein solutions (5 μM) containing complexes **1** – **3** with concentrations ranging from 50 to 300 μM were photo-irradiated at 365 nm (100 W UV lamp) for 30 min after 2 h incubation at 37 °C. Protein samples were evaporated under vacuum using EYELA Centrifugal Vaporizer (Model CVE-200D). The irradiated samples (50 μL) were dried in a centrifugal vaporizer and the samples were dissolved in the loading buffer (20 μL) containing SDS (7% w/v), glycerol (4% w/v), Tris-HCl buffer (50 mM, pH 6.8), mercaptoethanol (2% v/v) and bromophenol blue (0.01% w/v). The protein solutions were then denatured on heating to boil for 3 min. The samples were loaded on a 3% polyacrylamide (stacking) gel. The gel electrophoresis was done by applying 60 V until the dye passed into the separating gel from the stacking

(3%) gel and the voltage was increased to 120 V. The gels were run for 1.5 h followed by staining with Coomassie Brilliant Blue R-250 solution (acetic acid/methanol/water as 1:2:7 v/v) and destaining was done with water/methanol/acetic acid mixture (5:4:1 v/v) for 4 h. The gels were scanned with a HP Scanjet G3010 scanner and the images were processed using Adobe Photoshop. Molecular weight markers were used in each gel to calibrate the molecular weights of the BSA. The presence of reactive oxygen species was investigated by carrying out the photo-induced protein cleavage experiment in the presence of various additives like DABCO (3 mM), NaN_3 (3 mM), KI (3 mM) and DMSO (25 μL).

DAPI staining

Nuclear staining was performed as reported earlier.[10] Briefly, the HeLa cells after 3 h incubation with complex **3** were photoexposed to visible light (400-700 nm, 10 J cm^{-2}). After 2 h post-treatment the cells were washed with PBS and fixed in 3.7% paraformaldehyde for 10 min. The fixed cells were then permeabilized with TBST [50 mM Tris-HCl (pH 7.4), 150 mM NaCl, and 0.1% Triton X-100] for 5 min. Cells were washed with PBS and then a 4',6-diamidino-2-phenylindole (DAPI) solution (10 μg mL^{-1} in PBS) was added to the cells and kept for 5 min. After several washings with PBS, the cells were observed under a fluorescence microscope (Olympus IX-71) with 360/40 nm excitation and 460/50 nm emission filters to determine any condensed or fragmented nuclei indicating cells undergoing apoptosis.

References.

(1) C. Merill, D. Goldman, S. A. Sedman and M. H. Ebert, *Science*, 1980, **211**, 1437.

(2) M. E. Reichman, S. A. Rice, C. A. Thomas and P. Doty, *J. Am. Chem. Soc.* 1954, **76**, 3047.

(3) J. D. McGhee and P. H. von Hippel, *J. Mol. Biol.*, 1974, **86**, 469.

(4) M. T. Carter, M. Rodriguez and A. J. Bard, *J. Am. Chem. Soc.*, 1989, **111**, 8901.

(5) D. Thierry, *J. Photochem. Photobio. B.*, 2006, **82**, 45.

(6) S. Satyanarayana, J. C. Dabrowiak and J. B. Chaires, *Biochemistry*, 1992, **31**, 9319.

(7) J. Bernadou, G. Pratviel, F. Bennis, M. Girardet and B. Meunier, *Biochemistry*, 1989, **28**, 7268.

(8) Y.-J. Hu, Y. Liu, J.-B. Wang, X.-H. Xiaob and S. S. Qu, *J. Pharm. Biomed. Anal.*, 2004, **36**, 915.

(9) (a) C. V. Kumar, A. Buranaprapuk, G. J. Opiteck, M. B. Moyer, S. Jockusch and N. J. Turro, *Proc.Natl. Acad. Sci. USA*., 1998, **95**, 10361. (b) A. Buranaprapuk, S. P. Leach, C. V. Kumar and J. R. Bocarsly, *Biochim. Biophys. Acta.*, 1998, **1387**, 309.

(10) S. Park, S. P. Hong, T. Y. Oh, S. Bang, J. B. Chung, S. Y. Song, *Photochem. Photobiol. Sci.*, 2008, **7**, 769.

Full reference for Gaussian09 (reference number 59 in the text of the manuscript)

M. J. Frisch, G. W.Trucks, H. B. Schlegel, G. E. Scuseria, M. A. Robb, J. R. Cheeseman, G. Scalmani, V. Barone, B. Mennucci, G. A. Petersson, H. Nakatsuji, M. Caricato, X. Li, H. P. Hratchian, A. F. Izmaylov, J. Bloino, G. Zheng, J. L. Sonnenberg, M. Hada, M. Ehara, K. Toyota, R. Fukuda, J. Hasegawa, M. Ishida, T. Nakajima, Y. Honda, O. Kitao, H. Nakai, T. Vreven, J. A., Jr. Montgomery, J. E. Peralta, F. Ogliaro, M. Bearpark, J. J.

Heyd, E. Brothers, K. N. Kudin, V. N. Staroverov, R. Kobayashi, J. Normand, K. Raghavachari, A. Rendell, J. C. Burant, S. S. Iyengar, J. Tomasi, M. Cossi, N. Rega, J. M. Millam, M. Klene, J. E. Knox, J. B. Cross, V. Bakken, C. Adamo, J. Jaramillo, R. Gomperts, R. E. Stratmann, O. Yazyev, A. J. Austin, R. Cammi, C. Pomelli, J. W. Ochterski, R. L. Martin, K. Morokuma, V. G. Zakrzewski, G. A. Voth, P. Salvador, J. J. Dannenberg, S. Dapprich, A. D. Daniels, O. Farkas, J. B. Foresman, J. V. Ortiz, J. Cioslowski, D. J. Fox, Gaussian, Inc., Wallingford CT, 2009.

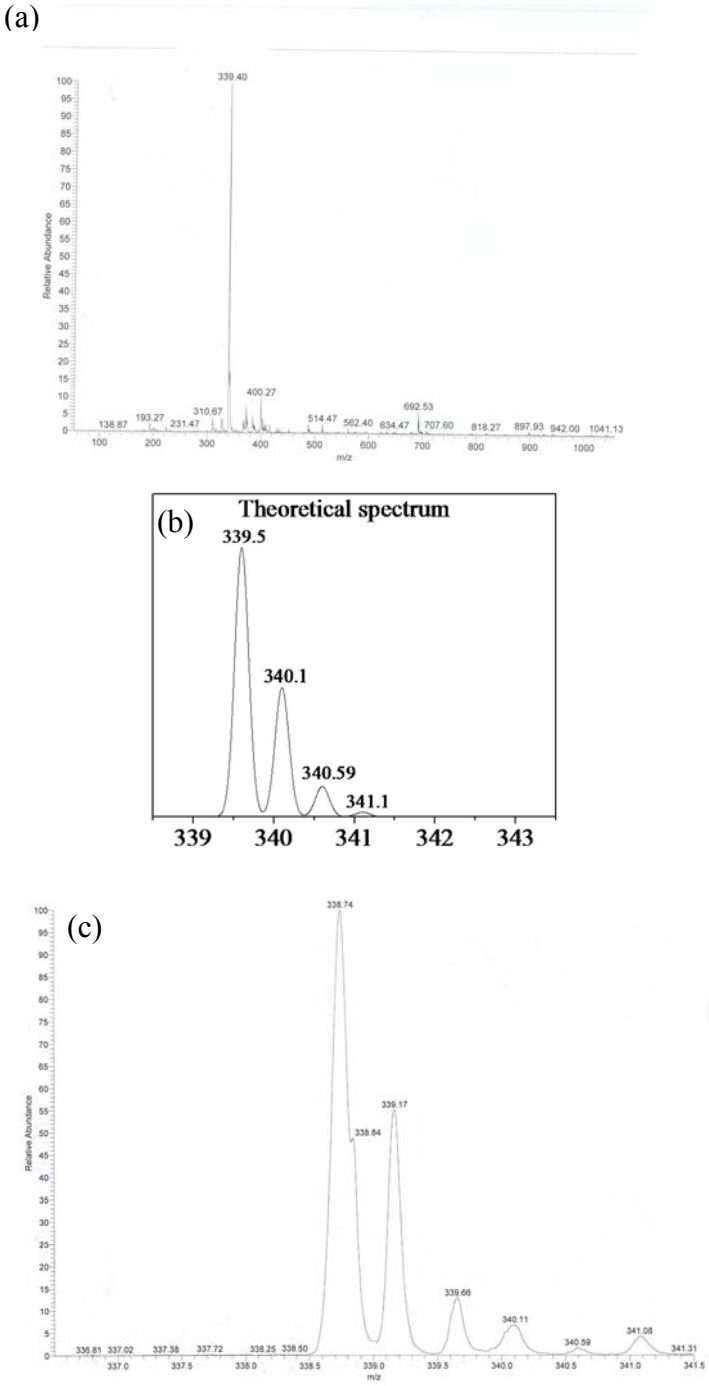

Fig. S1. (a) ESI-MS of $[Co(ph\text{-}tpy)_2](ClO_4)_2$ (**1**) in 10% aqueous methanol showing the parent ion peak. (b) The calculated spectrum of complex **1** showing the isotropic distribution pattern. (c) Experimental mass spectrum of complex **1** showing the isotropic distribution.

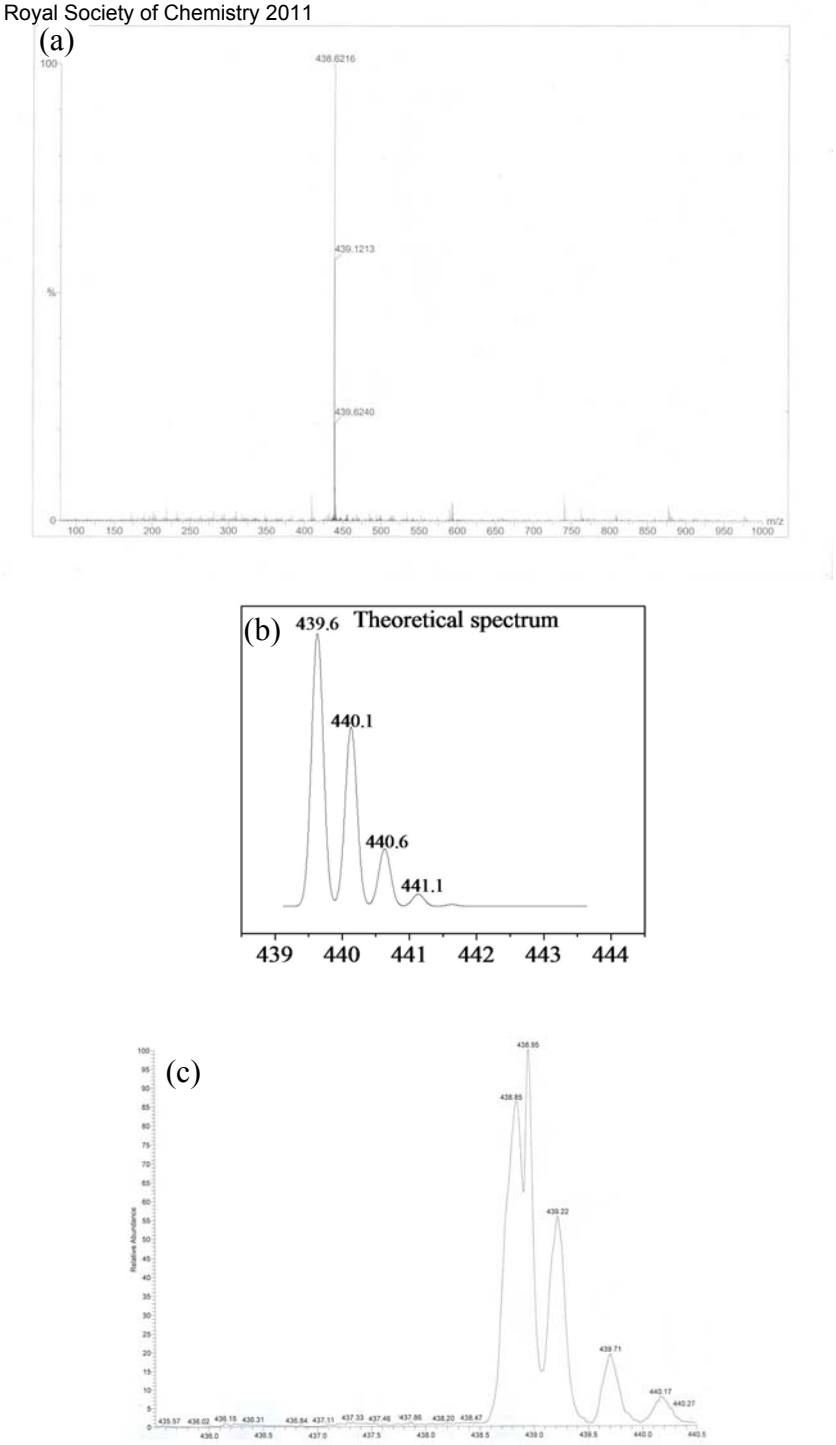

Fig. S2.(a) ESI-MS of $[Co(an\text{-}tpy)_2](ClO_4)_2$ (**2**) in 10% aqueous methanol showing the parent ion peak. (b) The calculated spectrum of complex **2** showing the isotropic distribution pattern. (c) Experimental mass spectrum of complex **2** showing the isotropic distribution.

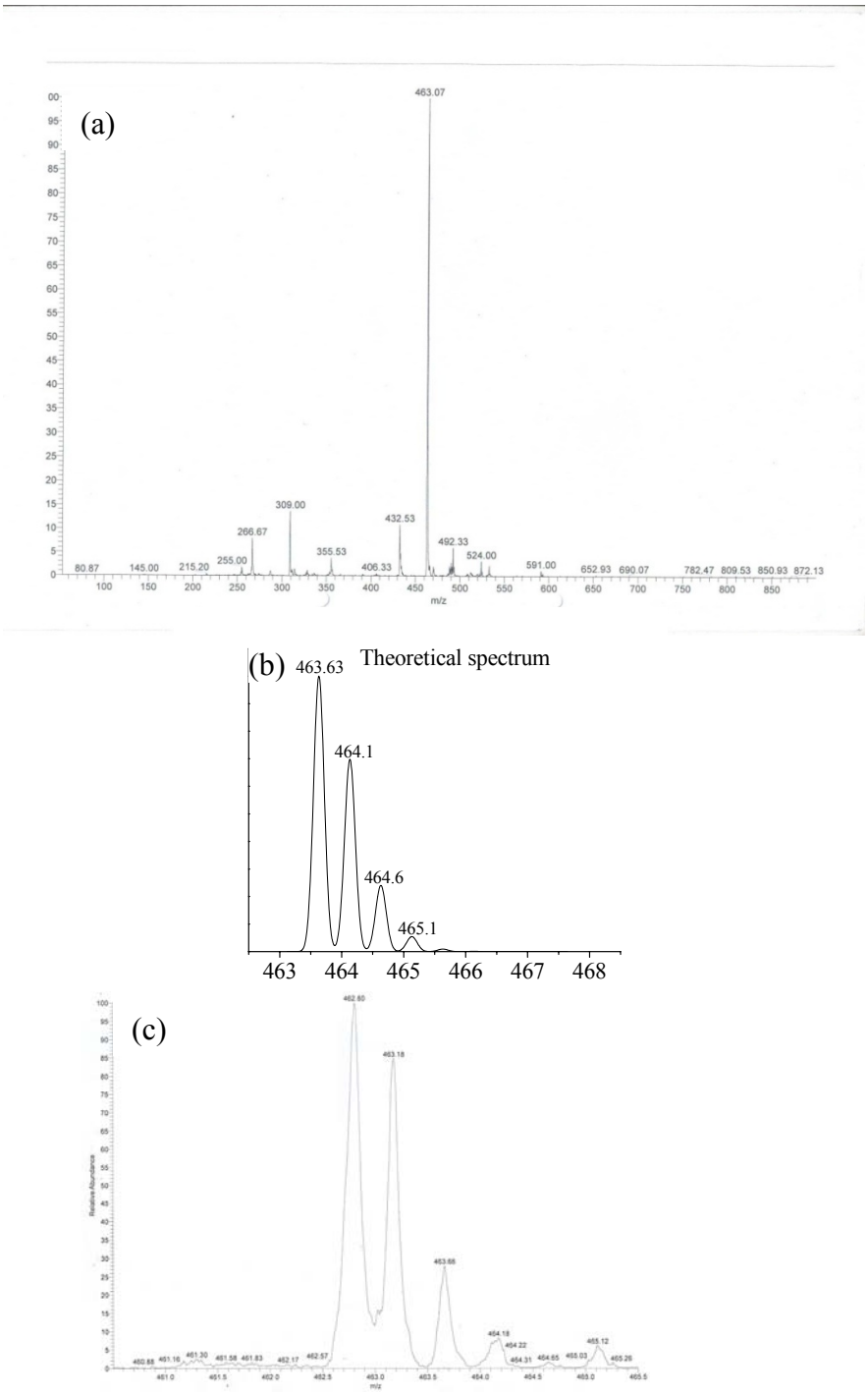

Fig. S3. (a) ESI-MS of $[Co(py\text{-}tpy)_2](ClO_4)_2$ (**3**) in 10% aqueous methanol showing the parent ion peak. (b) The calculated spectrum of complex **3** showing the isotropic distribution pattern. (c) Experimental mass spectrum of complex **3** showing the isotropic distribution.

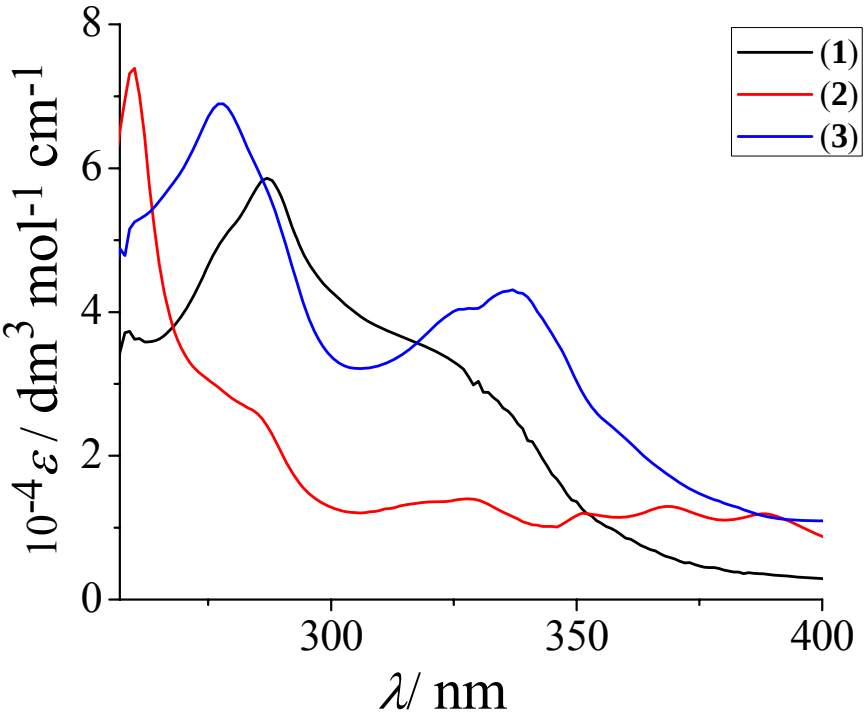

Fig. S4. Electronic spectra of $[Co(ph\text{-}tpy)_2](ClO_4)_2$ (**1**, black line), $[Co(an\text{-}tpy)_2](ClO_4)_2$ (**2**, red line) and $[Co(py\text{-}tpy)_2](ClO_4)_2$ (**3**, blue line) in DMF-H_2O (2:1 v/v).

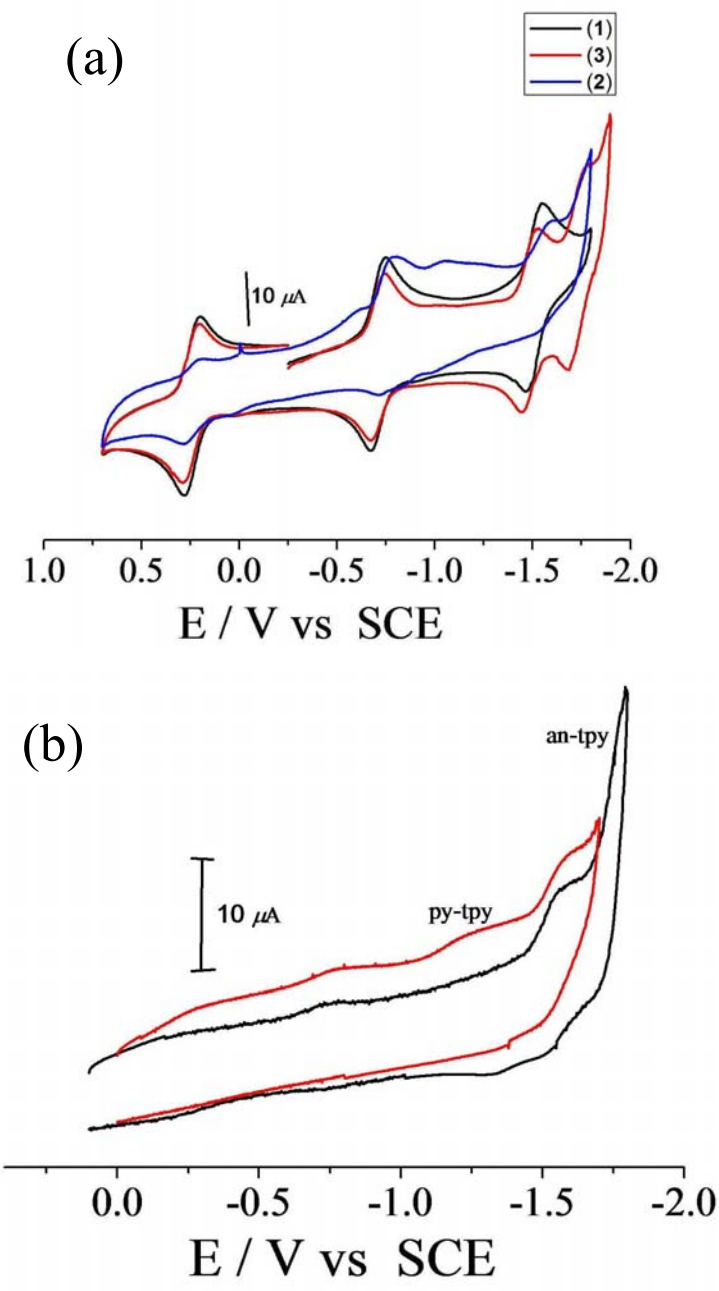

Fig. S5. (a) The cyclic voltammetric responses of $[Co(ph\text{-}tpy)_2](ClO_4)_2$ (**1**), $[Co(an\text{-}tpy)_2](ClO_4)_2$ (**2**) and $[Co(py\text{-}tpy)_2](ClO_4)_2$ (**3**) in DMF-0.1 M TBAP at a scan rate of 50 mV s^{-1}. (b) The cyclic voltammetric responses of the ligands an-tpy and py-tpy in DMF-0.1 M TBAP at a scan rate of 50 mV s^{-1}.

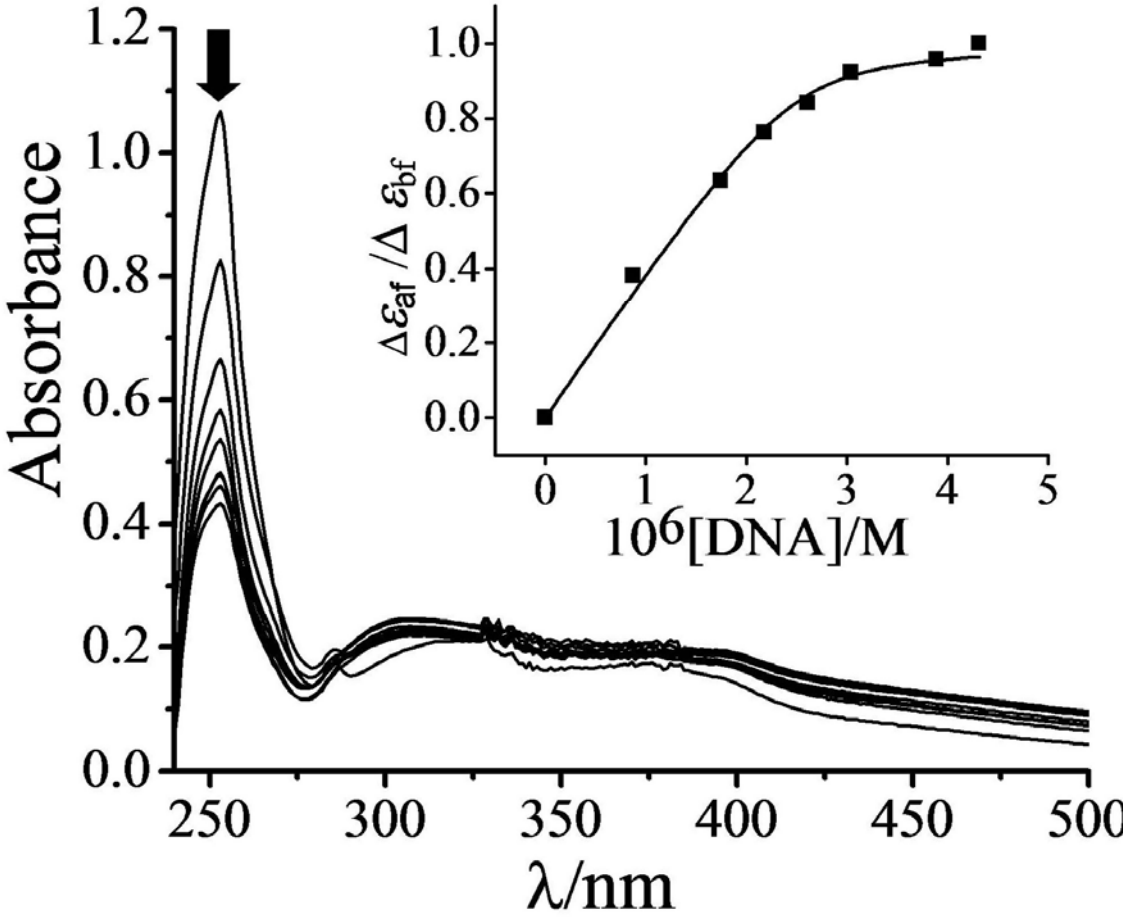

Fig. S6. Absorption spectral traces of $[Co(an\text{-}tpy)_2](ClO_4)_2$(**2**) on addition of CT DNA in a Tris-HCl buffer medium (pH 7.2). The inset shows the plot of $\Delta\varepsilon_{af}/\Delta\varepsilon_{bf}$ vs [DNA] obtained from absorption spectral titration of the complex **2** with CT-DNA in Tris-buffer (pH 7.2), where $\Delta\varepsilon_{af} = (\varepsilon_a - \varepsilon_f)$ and $\Delta\varepsilon_{bf} = (\varepsilon_b - \varepsilon_f)$.

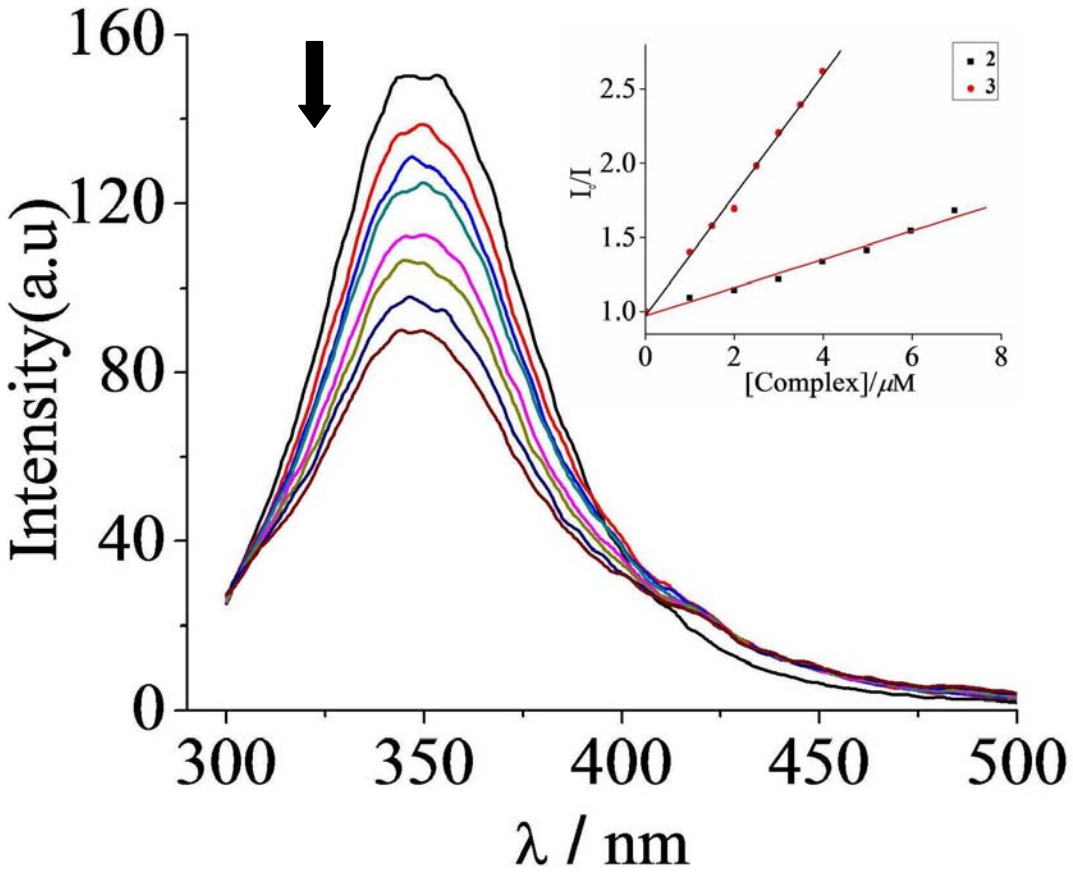

Fig. S7. Emission spectral trace of 2μM BSA protein in 5 mM phosphate buffer on increasing quantity of $[Co(an\text{-}tpy)_2](ClO_4)_2$ (**2**). The inset shows the plot of I_0/I *versus* [complex] for $[Co(an\text{-}tpy)_2](ClO_4)_2$ (**2**) and $[Co(py\text{-}tpy)_2](ClO_4)_2$ (**3**).

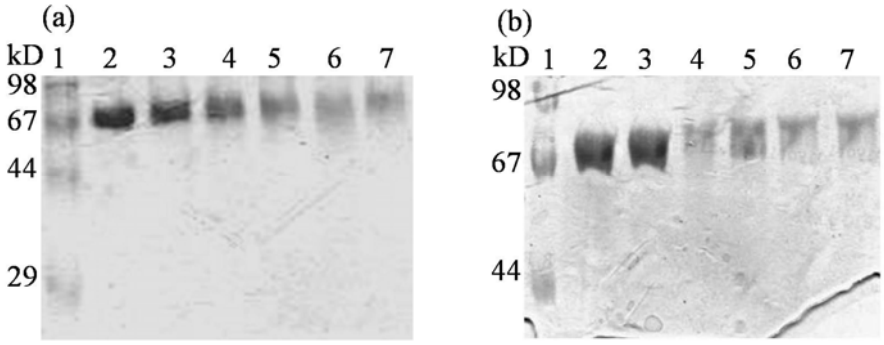

Fig. S8. SDS-PAGE diagram showing photocleavage of bovine serum albumin (BSA, 5 μM) in UV-A light of 365 nm (100 W lamp) by the complexes $[Co(an\text{-}tpy)_2](ClO_4)_2$ (**2**) and $[Co(py\text{-}tpy)_2](ClO_4)_2$ (**3**) for an exposure time of 45 min. Panels (a) and (b) are for the complexes **2** and **3**, respectively:

Panel (a): lane-1, molecular marker; lane-2, BSA control; lane-3, BSA + **2** (300 μM, dark); lane-4, BSA + **2** (50 μM); lane-5, BSA + **2** (100 μM); lane-6, BSA + **2** (200 μM); lane-7, BSA + **2** (300 μM).

Panel (b): lane-1, molecular marker; lane-2, BSA control; lane-3, BSA + **3** (300 μM, in dark); lane-4, BSA + **3** (50 μM); lane-5, BSA + **3** (100 μM); lane-6, BSA + **3** (200 μM); lane-7, BSA + **3** (300 μM).

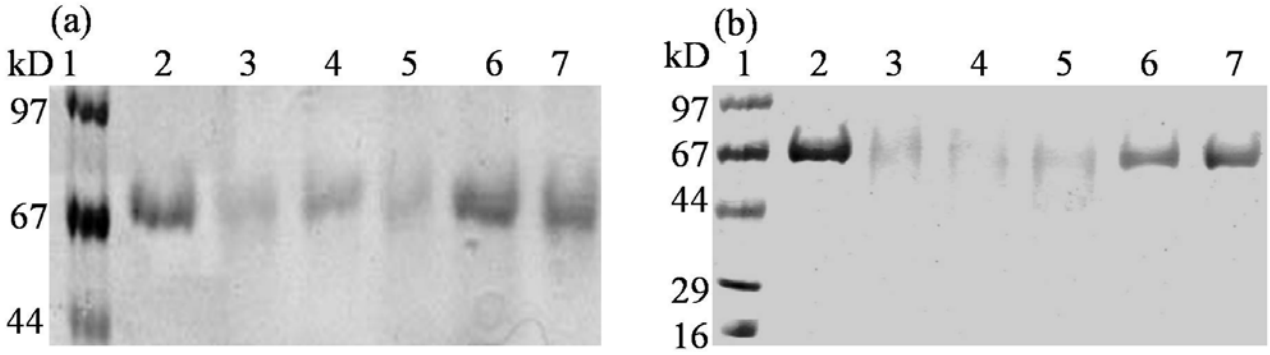

Fig. S9. SDS- PAGE diagram showing photocleavage of BSA protein (5 μM) in UV-A light of 365 nm by $[Co(an\text{-}tpy)_2](ClO_4)_2$ (**2**) and $[Co(py\text{-}tpy)_2](ClO_4)_2$ (**3**) in the presence of various additives for 45 min exposure time in 50 mM Tris-HCl /NaCl buffer (pH, 7.2). Panels (a) and (b) are for the complexes **2** and **3**, respectively:

Panel (a): lane-1, molecular marker; lane-2, BSA + **2** (300 μM, dark); lane-3, BSA + **2** (300 μM); lane-4, BSA + **2** (300 μM) + NaN_3 (3 mM); lane-5, BSA + **2** (300 μM) + DABCO (3 mM); lane-6, BSA + **2** (300 μM) + DMSO (20 μL); lane-7, BSA + **2** (300 μM) + KI (3 mM).

Panel (b): lane-1, molecular marker; lane-2, BSA + **3** (300 μM, dark); lane-3, BSA + **3** (300 μM); lane-4, BSA + **3** (300 μM) + NaN_3 (3 mM); lane-5, BSA + **3** (300 μM) + DABCO (3 mM).; lane-6, BSA + **3** (300 μM) + DMSO (20 μL); lane-7, BSA + **3** (300 μM) + KI (3 mM).

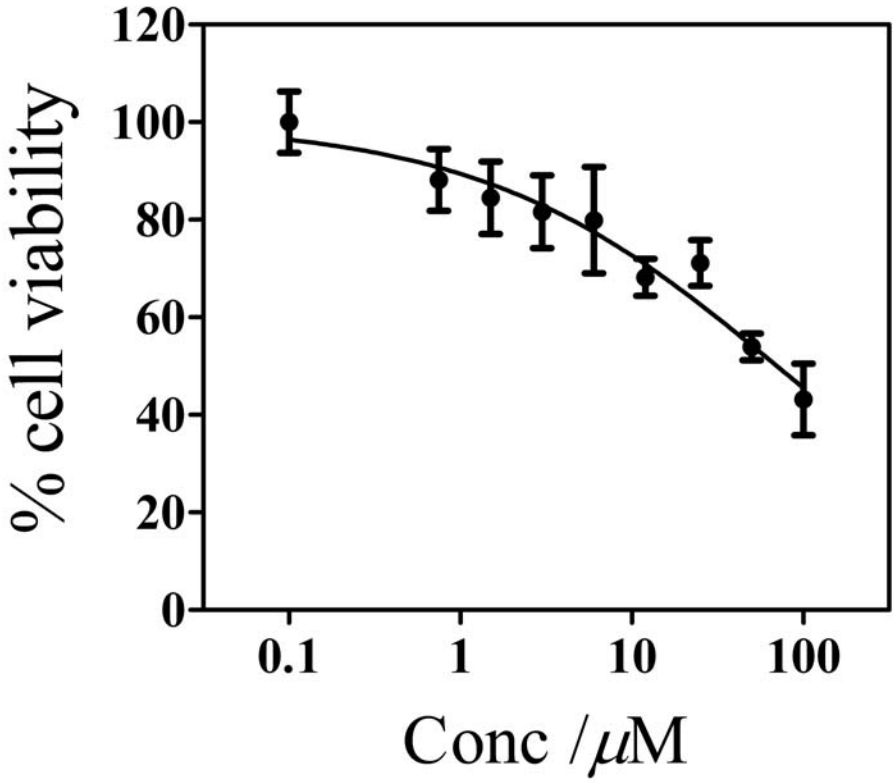

Fig. S10. MTT assay showing the toxicity of Cisplatin for 4 h incubation time in dark.

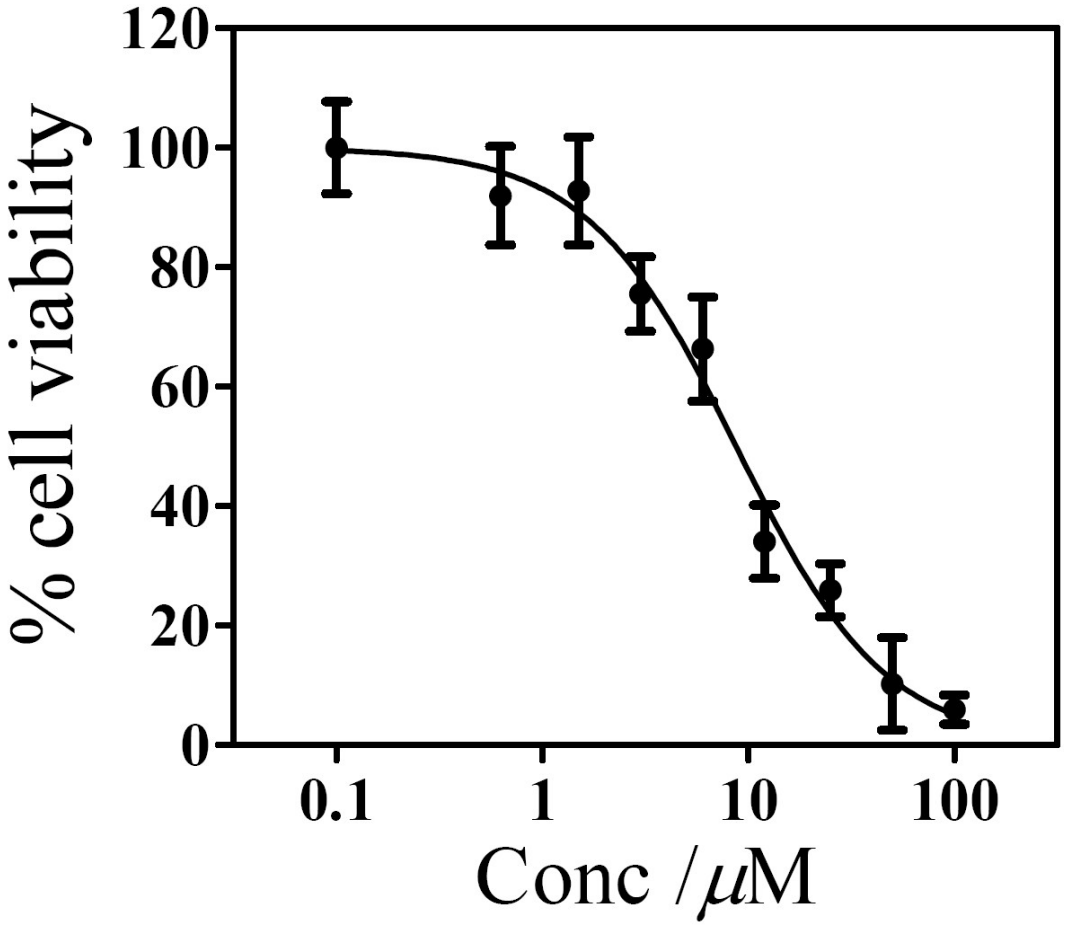

Fig. S11. MTT assay showing the toxicity of Cisplatin for 24 h incubation time in dark.

Table S1: Calculated transition energies (in nm), oscillator strengths (f), the major contributions and nature of each transition of complex **1**[a] with weight percentage at UB3LYP/LANL2DZ level of theory. The calculated transition energies of the free ph-tpy ligand are shown in parenthesis**.** All ILCT transitions are of $\pi \rightarrow \pi^*$ nature.

Transition energy	Oscillator strength	Excitation (weight)	Nature
593	0.0001	163B→180B (48%) 161B→181B (11%) 163B→178B (9%)	M→M
472	0.0055	168B→169B (30%) 170A→173A (15%) 171A→172A (16%) 167B→170B (14%)	LMCT
413	0.0340	168B→169B (22%) 165A→175A (12%) 164A→174A (12%)	LMCT
332 (281)	0.0575	162B→169B (46%) 164A→172A (8%) 161B→170B (8%)	LMCT
278 (251)	0.0845	170A→177A (30%) 171A→176A (13%)	ILCT

[a]HOMO=168B, LUMO=169B (β),
HOMO=171A, LUMO=172A (α)

Table S2: Calculated transition energies (in nm), oscillator strengths (f), the major contributions and nature of each transition of complex **2**[a] with weight percentage at UB3LYP/LANL2DZ level of theory. The calculated transition energies of the free an-tpy ligand are shown in parenthesis**.** All ILCT transitions are of $\pi \rightarrow \pi^*$ nature.

Transition energy	Oscillator strength	Excitation (weight)	Nature
541	0.0005	214B→235B (47%) 214B→233B (10%) 213B→232B (5%)	M→M
436	0.0011	223A→231A (55%) 220B→228B (15%) 223A→230A (12%)	ILCT
399 (387)	0.0040	223A→233A (28%) 220B→231B (23%) 222A→232A (17%)	ILCT
367 (347)	0.0152	219A→226A (56%) 219A→227A (31%)	ILCT
351 (351)	0.0015	223A→234A (28%) 220B→233B (25%) 220B→234B (22%)	ILCT
340	0.0042	213B→222B (40%) 211B→222B (20%)	MLCT
291 (285)	0.0357	212B→223B (37%) 205B→221B (9%)	ILCT
279 (256)	0.0643	215A→224A (8%) 216B→226B (6%) 219A→229A (5%)	ILCT

[a]HOMO=220B, LUMO=221B (β),
HOMO=223A, LUMO=224A (α).

Table S3: Calculated transition energies (in nm), oscillator strengths (f), the major contributions and nature of each transition of complex **3**[a] with weight percentage at UB3LYP/LANL2DZ level of theory. The calculated transition energies of the free py-tpy ligand are shown in parenthesis**.** All ILCT transitions are of $\pi \rightarrow \pi^*$ nature.

Transition energy	Oscillator strength	Excitation (weight)	Nature
544	0.0001	224B→245B (47%) 226B→245B (6%) 227B→240B (5%)	M→M
508 (358)	0.0009	232B→237B (83%) 231B→237B (11%)	LMCT
408 (338)	0.0015	232B→241B (95%)	LMCT
341 (312)	0.0382	223B→234B (31%) 225B→234B (16%)	MLCT
324 (278)	0.0066	228A→237A (24%) 226A→238A (18%)	ILCT
276 (252)	0.0573	230A→242A (16%) 227B→239B (15%) 227B→240B (11%)	ILCT

[a]HOMO=232B, LUMO=233B (β),
HOMO=235A, LUMO=236A (α).